

## SCALAR AND VECTOR TIME SERIES METHODS FOR VIBRATION BASED DAMAGE DIAGNOSIS IN A SCALE AIRCRAFT SKELETON STRUCTURE

FOTIS P. KOPSAFTOPOULOS  
SPILIOS D. FASSOIS

*University of Patras, Department of Mechanical and Aeronautical Engineering, Patras, Greece*  
*e-mail: fkopsaf@mech.upatras.gr; fassois@mech.upatras.gr*

A comparative assessment of several scalar and vector statistical time series methods for vibration based Structural Health Monitoring (SHM) is presented via their application to a laboratory scale aircraft skeleton structure in which different damage scenarios correspond to the loosening of different bolts. A concise overview of scalar and vector methods, that is methods using scalar or vector signals, statistics, and corresponding models, is presented. The methods are further classified as non-parametric or parametric and response-only or excitation-response. The effectiveness of the methods for both damage detection and identification is assessed via various test cases corresponding to different damage scenarios. The results of the study reveal various facets of the methods and confirm the global damage diagnosis capability and the effectiveness of both scalar and vector statistical time series methods for SHM.

*Key words:* Structural Health Monitoring (SHM), damage detection, damage identification

### Acronyms

ARMA – AutoRegressive Moving Average, ARX – AutoRegressive with eXogenous excitation, BIC – Bayesian Information Criterion, FRF – Frequency Response Function, iid – identically independently distributed, LS – Least Squares, PE – Prediction Error, PSD – Power Spectral Density, RSS – Residual Sum of Squares, SHM – Structural Health Monitoring, SPP – Samples Per Parameter, SPRT – Sequential Probability Ratio Test, SSS – Signal Sum of Squares.

## 1. Introduction

Statistical time series methods for damage detection and identification (localization), collectively referred to as damage diagnosis, utilize random excitation and/or vibration response signals (time series) along with statistical model building and decision making tools for inferring the health state of a structure (Structural Health Monitoring – SHM). They offer a number of advantages, including no requirement for physics based or finite element models, no requirement for complete modal models, effective treatment of uncertainties, and statistical decision making with specified performance characteristics (Fassois and Sakellariou, 2007, 2009). These methods form an important, rapidly evolving category within the broader family of vibration based methods (Doebbling *et al.*, 1998; Sakellariou and Fassois, 2008; Kopsaftopoulos and Fassois, 2010).

Statistical time series methods for SHM are based on *scalar* or *vector* random (stochastic) vibration signals under healthy and potentially damaged structural states, identification of suitable (parametric or non-parametric) time series models describing the dynamics under each structural state, and extraction of a statistical characteristic quantity  $Q_o$  characterizing the structural state in each case (baseline phase). Damage diagnosis is then accomplished via statistical decision making consisting of comparing, in a statistical sense, the current characteristic quantity  $Q_u$  with that of each potential state as determined in the baseline phase (inspection phase). For an extended overview of the basic principles and the main statistical time series methods for SHM, the interested reader is referred to Fassois and Sakellariou (2007, 2009). An experimental assessment of several methods is provided in Kopsaftopoulos and Fassois (2010).

*Non-parametric* time series methods are those based on corresponding scalar or vector non-parametric time series representations such as spectral estimates (Power Spectral Density, Frequency Response Function) (Fassois and Sakellariou, 2007, 2009), and have received limited attention in the literature (Sakellariou *et al.*, 2001; Liberatore and Carman, 2004; Hwang and Kim, 2004; Rizos *et al.*, 2008; Kopsaftopoulos and Fassois, 2010). On the other hand, *parametric* time series methods are those based on corresponding scalar or vector parametric time series representations such as the AutoRegressive Moving Average (ARMA) models (Fassois and Sakellariou, 2007, 2009). This latter category has attracted significant attention recently, and their principles have been used in a number of studies (Sohn and Farrar, 2001; Sohn *et al.*, 2001, 2003; Basseville *et al.*, 2004; Sakellariou and Fassois, 2006;

Nair *et al.*, 2006; Mattson and Pandit, 2006; Zheng and Mita, 2007; Carden and Brownjohn, 2008; Gao and Lu, 2009; Kopsaftopoulos and Fassois, 2010).

The *goal* of the present study is the comparative assessment of several *scalar* (univariate) and *vector* (multivariate) statistical time series methods for SHM via their application to an aircraft scale skeleton structure in which different damage scenarios correspond to the loosening of different bolts. The methods are further classified as non-parametric or parametric and response-only or excitation-response. Preliminary results by various methods may be found in our recent papers (Kopsaftopoulos *et al.*, 2010; Kopsaftopoulos and Fassois, 2011). It should be noted that the structure has been used in the past for the development of novel scalar (univariate) methods for precise damage localization and magnitude (size) estimation using different (simulated) damages consisting of small masses attached to the structure (Sakellariou and Fassois, 2008; Kopsaftopoulos and Fassois, 2007). Due to their ability to address the precise localization and magnitude estimation problems, these methods are generally more complex. As the focus of the present study is more on damage detection and identification (the latter in the sense of estimating the damage scenario from a given pool of potential scenarios), only simpler methods are utilized.

More specifically, four scalar methods, namely the Power Spectral Density (PSD), Frequency Response Function (FRF), model residual variance, and Sequential Probability Ratio Test (SPRT) based method are employed, along with two vector methods, namely the model parameter based and residual likelihood function based method. A number of test cases (experiments) are considered, each one corresponding to a specific damage scenario (loosening of one or more bolts connecting various structural elements).

The main issues addressed in the study are:

- (a) Assessment of the methods in terms of their damage detection capability under various damage scenarios and different vibration measurement locations (classified as either “local” or “remote” to damage location).
- (b) Comparison of the performance characteristics of *scalar* and *vector* statistical time series methods with respect to effective damage diagnosis: false alarm, missed damage and damage misclassification rates are investigated.
- (c) Assessment of the ability of the methods to accurately identify (classify) the damage type through “local” or “remote” sensors.

## 2. The structure and the experimental set-up

### 2.1. The structure

The scale aircraft skeleton structure used in the experiments was designed by ONERA (France) in conjunction with the Structures and Materials Action Group SM-AG19 of the Group for Aeronautical Research and Technology in Europe (GARTEUR) (Degener and Hermes, 1996; Balmes and Wright, 1997) and manufactured at the University of Patras (Fig. 1). It represents a typical aircraft skeleton design and consists of six solid beams with rectangular cross sections representing the fuselage ( $1500 \times 150 \times 50$  mm), the wing ( $2000 \times 100 \times 10$  mm), the horizontal ( $300 \times 100 \times 10$  mm) and vertical stabilizers ( $400 \times 100 \times 10$  mm) and the right and left wing-tips ( $400 \times 100 \times 10$  mm). All parts are made of standard aluminum and are jointed together via steel plates and bolts. The total mass of the structure is approximately 50 kg.

### 2.2. The damage scenarios and the experiments

Damage detection and identification is based on vibration testing of the structure, which is suspended through a set of bungee cords and hooks from a long rigid beam sustained by two heavy-type stands (Fig. 1). The suspension is designed in a way as to exhibit a pendulum rigid body mode below the frequency range of interest, as the boundary conditions are free-free.

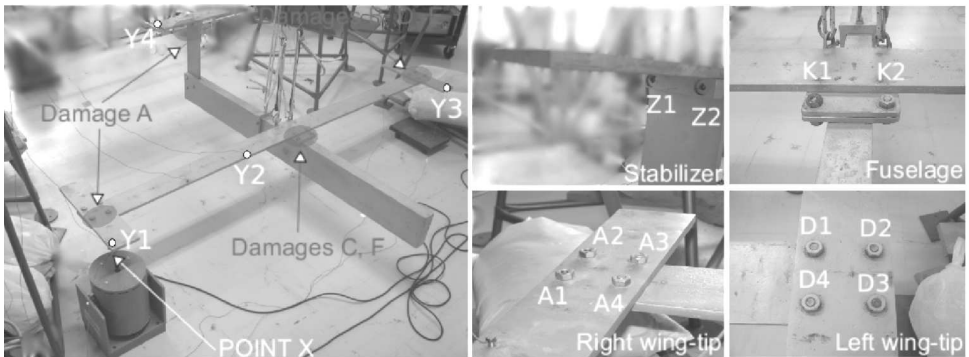


Fig. 1. The scale aircraft skeleton structure and the experimental set-up: The force excitation (Point X), vibration measurement locations (Points Y1-Y4), and bolts connecting various elements of the structure

The excitation is broadband random stationary Gaussian force applied vertically at the right wing-tip (Point X, Fig. 1) through an electromechanical shaker (MB Dynamics Modal 50A, max load 225 N). The actual force exerted

on the structure is measured via an impedance head (PCB M288D01, sensitivity 98.41 mV/lb), while the resulting vertical acceleration responses at Points Y1, Y2, Y3 and Y4 (Fig. 1) are measured via lightweight accelerometers (PCB 352A10 miniature ICP accelerometers, 0.7 g, frequency range 0.003-10 kHz, sensitivity  $\sim 1.052$  mV/m/s<sup>2</sup>). The force and acceleration signals are driven through a conditioning charge amplifier (PCB 481A02) into the data acquisition system based on two SigLab 20-42 measurement modules (each module featuring four 20-bit simultaneously sampled A/D channels, two 16-bit D/A channels, and analog anti-aliasing filters).

The damage scenarios considered correspond to the loosening of various bolts at different joints of the structure (Fig. 1). Six distinct scenarios (types) are considered and summarized in Table 1. The assessment of the presented statistical time series methods with respect to the damage detection and identification subproblems is based on 60 experiments for the healthy and 40 experiments for each considered damage state of the structure (damage types A, B, . . . , F – see Table 1) – each experiment corresponding to a single test case. Moreover, *four* vibration measurement locations (Fig. 1, Points Y1-Y4) are employed in order to determine the ability of the considered methods in treating damage diagnosis using single or multiple vibration response signals. The frequency range of interest is selected as 4-200 Hz with the lower limit set in order to avoid instrument dynamics and rigid body modes. Each signal is digitized at  $f_s = 512$  Hz and is subsequently sample mean corrected and normalized by its sample standard deviation (Table 1).

**Table 1.** The damage scenarios and experimental details

Structural state	Description	No of inspection experiments (test cases)
Healthy	–	60
Damage A	loosening of bolts A1, A4, Z1, Z2	40
Damage B	loosening of bolts D1, D2, D3	40
Damage C	loosening of bolts K1	40
Damage D	loosening of bolts D2, D3	40
Damage E	loosening of bolts D3	40
Damage F	loosening of bolts K1, K2	40
Sampling frequency: $f_s = 512$ Hz, Signal bandwidth: 4-200 Hz		
Signal length in samples (s):		
Non-parametric methods: $N = 46\,080$ (90 s)		
Parametric methods: $N = 15\,000$ (29 s)		

A single healthy data set is used for establishing the baseline (reference) set, while 60 healthy and 240 damage sets (six damage types with 40 experiments each) are used as inspection data sets. For damage identification, a single data set for each damage structural state (damage types A, B, . . . , F) is used for establishing the baseline (reference) set, while the same 240 sets are considered as inspection data sets (each corresponding to the test case in which the actual structural state is considered unknown). The time series models are estimated and the corresponding estimates of the characteristic quantity  $Q$  are extracted ( $\widehat{Q}_A, \widehat{Q}_B, \dots, \widehat{Q}_F$  in the baseline phase;  $\widehat{Q}_u$  in the inspection phase). Damage identification is presently based on successive binary hypothesis tests – as opposed to multiple hypothesis tests – and should be thus considered as preliminary (Fassois and Sakellariou, 2009).

### 3. Structural dynamics of the healthy structure

#### 3.1. Non-parametric identification

Non-parametric identification of the structural dynamics is based on  $N = 46\,080$  ( $\approx 90$  s) sample-long excitation-response signals obtained from *four* vibration measurement locations on the structure (see Fig. 1). An  $L = 2\,048$  sample-long Hamming data window with zero overlap is used (number of segments  $K = 22$ ) for PSD (MATLAB function *pwelch.m*) and FRF (MATLAB function *tfestimate.m*) Welch based estimation (see Table 2).

**Table 2.** Non-parametric estimation details

Data length	$N = 46\,080$ samples ( $\approx 90$ s)
Method	Welch
Segment length	$L = 2\,048$ samples
Non-overlapping segments	$K = 22$ segments
Window type	Hamming
Frequency resolution	$\Delta f = 0.355$ Hz

The obtained FRF magnitude estimates for the healthy and damage states of the structure for the Point X - Point Y2 transfer function are depicted in Fig. 2. As it may be observed, the FRF magnitude curves are quite similar in the 4-60 Hz range; notice that this range includes the first five modes of the structure. Significant differences between the healthy and damage type A, C and F magnitude curves are observed in the range of 60-150 Hz, where the

next four modes are included. Finally, in the range of 150-200 Hz another two modes are present and discrepancies are more evident for damage types A, B, C and F. Notice that the FRF magnitude curves for damage types D and E are very similar to those of the healthy structure.

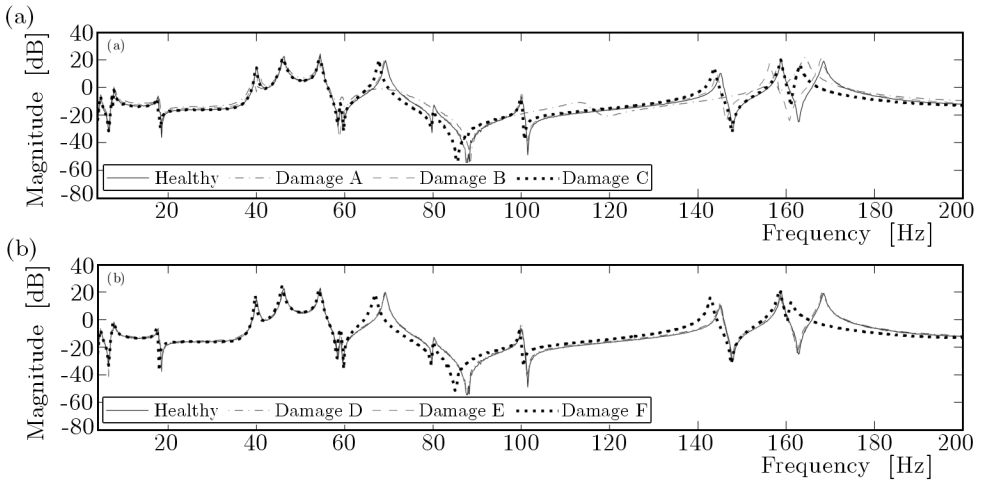


Fig. 2. Non-parametric Welch-based Frequency Response Function (FRF) magnitude estimates for the healthy and damaged structural states (Point X - Point Y2 transfer function)

### 3.2. Parametric identification

Parametric identification of the structural dynamics is based on  $N = 15\,000$  ( $\approx 29$  s) sample-long excitation and vibration response signals used in the estimation of Vector AutoRegressive with eXogenous excitation (VARX) models (MATLAB function *arx.m*). The modeling strategy consists of the successive fitting of VARX( $na, nb$ ) models (with  $na, nb$  designating the AR and X orders, respectively;  $na = nb = n$  is currently used) until a candidate model is selected. Model parameter estimation is achieved by minimizing a quadratic Prediction Error (PE) criterion (trace of the residual covariance matrix) leading to a Least Squares (LS) estimator (Fassois, 2001; Ljung, 1999, p. 206). Model order selection, which is crucial for successful identification, may be based on a combination of tools including the Bayesian Information Criterion (BIC) (Fig. 3), which is a statistical criterion that penalizes model complexity (order) as a counteraction to a decreasing model fit criterion (Fassois, 2001; Ljung, 1999, pp. 505-507) and the use of “stabilization diagrams” which depict the estimated modal parameters (usually frequencies) as a function

of the increasing model order (Fassois, 2001). BIC minimization is achieved for the model order  $n = 80$  (Fig. 3), thus a 4-variate VARX(80,80) model is selected as adequate for the residual variance, model parameter, and likelihood function based methods. The identified VARX(80,80) representation has  $d = 1604$  parameters, yielding a Sample Per Parameter (SPP) ratio equal to 37.4 ( $N \times (\text{no of outputs})/d$ ).

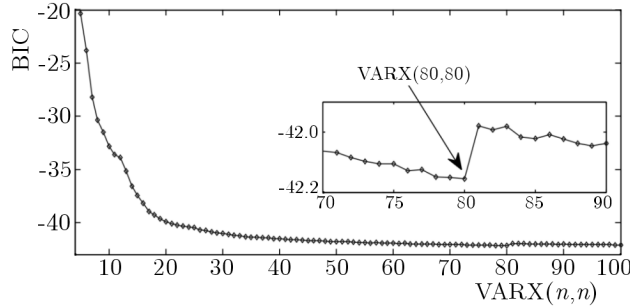


Fig. 3. Bayesian Information Criterion (BIC) for VARX( $n, n$ ) type parametric models in the healthy case

It should be noted that the complete 4-variate VARX(80,80) model is employed in conjunction with vector methods in Section 5. Yet, scalar parts of this model corresponding to excitation – single response are used in conjunction with scalar methods in Section 4. This is presently done for purposes of simplicity and it is facilitated by the fact that only a single (scalar) excitation is present.

#### 4. Scalar time series methods and their application

Scalar statistical time series methods for SHM employ *scalar* (univariate) models and corresponding statistics. In this Section, two non-parametric scalar methods, namely a Power Spectral Density (PSD) based method and a Frequency Response Function (FRF) based method, and two parametric scalar methods, namely a residual variance based method and Sequential Probability Ratio Test (SPRT) based method, are briefly presented and then applied to the scale aircraft skeleton structure. Their main characteristics are summarized in Table 3.

##### 4.1. The Power Spectral Density (PSD) based method

Damage detection and identification is in this case tackled via characteristic changes in the Power Spectral Density (PSD)  $S(\omega)$  of the measured vibration

**Table 3.** Characteristics of the employed statistical time series methods for SHM

Method	Principle	Test Statistic	Type
PSD based	$S_u(\omega) \stackrel{?}{=} S_o(\omega)$	$F = \widehat{S}_o(\omega)/\widehat{S}_u(\omega) \sim F(2K, 2K)$	scalar
FRF based	$\delta H(j\omega)  =  H_o(j\omega)  -  H_u(j\omega)  \stackrel{?}{=} 0$	$Z =  \delta \widehat{H}(j\omega)  /\sqrt{2\widehat{\sigma}_H^2(\omega)} \sim N(0, 1)$	scalar
Residual variance	$\sigma_{ou}^2 \stackrel{?}{\leq} \sigma_{oo}^2$	$F = \widehat{\sigma}_{ou}^2/\widehat{\sigma}_{oo}^2 \sim F(N, N - d)$	scalar
SPRT based	$\sigma_{ou} \stackrel{?}{\leq} \sigma_o$ or $\sigma_{ou} \stackrel{?}{\geq} \sigma_1$	$\mathcal{L}(n) = n \log \frac{\sigma_o}{\sigma_1} + \frac{\sigma_1^2 - \sigma_o^2}{2\sigma_o^2\sigma_1^2} \sum_{t=1}^n e^2[t]$	scalar
Model parameter	$\delta\boldsymbol{\theta} = \boldsymbol{\theta}_o - \boldsymbol{\theta}_u \stackrel{?}{=} \mathbf{0}$	$\chi_{\hat{\boldsymbol{\theta}}}^2 = \delta\widehat{\boldsymbol{\theta}}^\top (2\widehat{\mathbf{P}}_\theta)^{-1} \delta\widehat{\boldsymbol{\theta}} \sim \chi^2(d)$	vector
Residual likelihood	$\boldsymbol{\theta}_o \stackrel{?}{=} \boldsymbol{\theta}_u$	$\sum_{t=1}^N (\mathbf{e}_{ou}^\top[t, \boldsymbol{\theta}_o] \cdot \boldsymbol{\Sigma}_o \cdot \mathbf{e}_{ou}[t, \boldsymbol{\theta}_o]) \leq l$	vector
<p>Explanation of Symbols:</p> <p><math>S(\omega)</math>: Power Spectral Density (PSD) function; <math> H(j\omega) </math>: Frequency Response Function (FRF) magnitude</p> <p><math>\sigma_H^2(\omega) = \text{var} [ \widehat{H}_o(j\omega) ]</math>; <math>\boldsymbol{\theta}</math>: model parameter vector; <math>d</math>: parameter vector dimensionality; <math>\mathbf{P}_\theta</math>: covariance of <math>\boldsymbol{\theta}</math></p> <p><math>\sigma_{oo}^2</math>: variance of residual signal obtained by driving the healthy structure signals through the healthy model</p> <p><math>\sigma_{ou}^2</math>: variance of residual signal obtained by driving the current structure signals through the healthy model</p> <p><math>\mathbf{e}_{ou}[t, \boldsymbol{\theta}_o]</math>: vector residual sequence obtained by driving the current structure signals through the healthy model</p> <p><math>\sigma_o, \sigma_1</math>: user defined values for the residual standard deviation under healthy and damage states, respectively</p> <p><math>\mathbf{e}</math>: <math>k</math>-variate residual sequence; <math>\boldsymbol{\Sigma}</math>: residual covariance matrix; <math>l</math>: user defined threshold</p> <p>The subscripts “<math>o</math>” and “<math>u</math>” designate the healthy and current (unknown) structural states, respectively</p>			

response signals (non-parametric method) as the excitation is assumed unavailable (*response-only method*). Thus, the characteristic quantity is  $Q = S(\omega)$  ( $\omega$  designates frequency – see Table 3). Damage detection is based on confirmation of statistically significant deviations (from the nominal/healthy) in the current structure’s PSD function at some frequency (Fassois and Sakellariou, 2007, 2009). Damage identification may be achieved by performing hypothesis testing similar to the above separately for damages of each potential type. It should be noted that response signal scaling is important in order to properly account for potentially different excitation levels.

**Application Results.** Typical non-parametric damage detection results using the vibration measurement location of Point Y1 are presented in Fig. 4. Evidently, correct detection at the  $\alpha = 10^{-4}$  risk level is obtained in each case as the test statistic is shown not to exceed the critical point (dashed horizontal

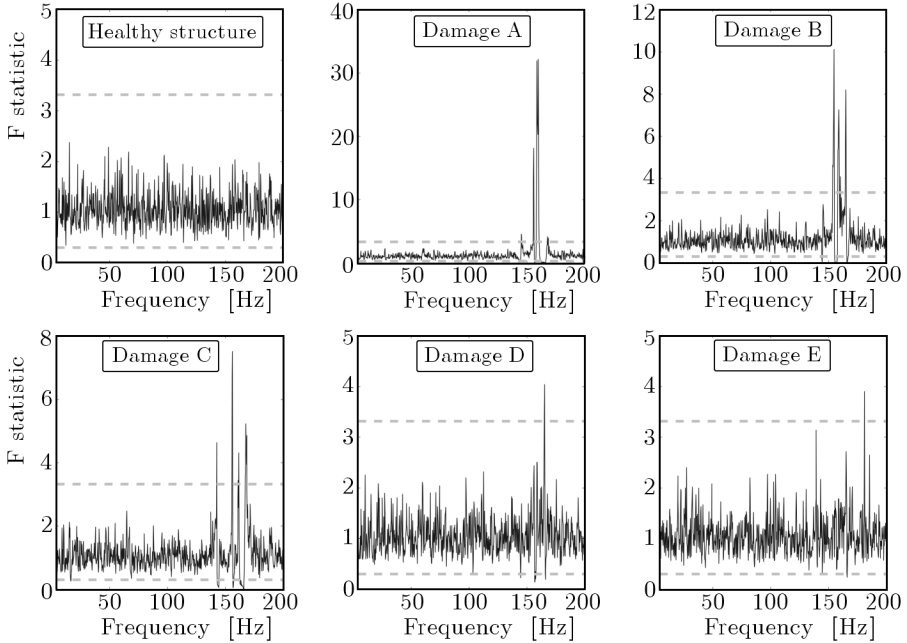


Fig. 4. PSD based method: Representative damage detection results (sensor Y1) at the  $\alpha = 10^{-4}$  risk level. The actual structural state is shown inside each plot

lines) in the healthy test case, while it exceeds it in each damage test case. Observe that damage types A, B and C (see Fig.1 and Table 1) are more easily detectable (note the logarithmic scale on the vertical axis of Fig.4), while damage types D and E are harder to detect. This is in agreement with

the remarks made in Subsection 3.1. Furthermore, notice that the frequency bandwidth of [150-170] Hz is more sensitive to damage. This is also in agreement with the remarks made in Subsection 3.1 and seems to be due to the fact that the two natural frequencies in this bandwidth are more sensitive to the considered damage scenarios (see Fig. 2).

Representative damage identification results at the  $\alpha = 10^{-4}$  risk level and using (as an example) the vibration measurement location at Point Y3 are presented in Fig. 5, with the actual damage being of type A. The test statistic does not exceed the critical point when the Damage A hypothesis is considered, while it exceeds it in all remaining cases. This correctly identifies damage type A as the current underlying damage.

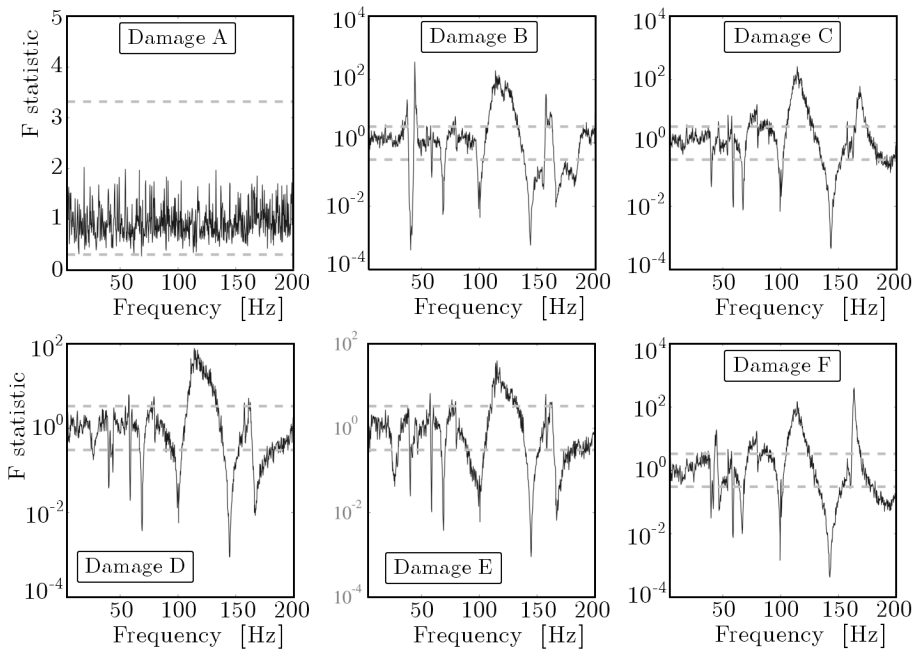


Fig. 5. PSD based method: Representative damage identification results (sensor Y3) at the  $\alpha = 10^{-4}$  risk level with the actual damage being of type A. Each considered damage hypothesis is shown inside each plot

Summary damage detection and identification results for each vibration measurement location (Fig. 1) are presented in Table 4. The PSD based method achieves accurate damage detection as no false alarms are exhibited, while the number of missed damage cases is zero for all considered damaged structural states. The method is also capable of identifying the actual damage type, as zero damage misclassification errors are reported for damage types A,

C, D and F, while it exhibits some misclassification errors for damage type E. The misclassification problem is more intense for damage type B when either the Y3 or the Y4 vibration measurement location is used (Table 4).

**Table 4.** Scalar methods: damage detection and identification summary results

Method	Damage Detection						
	False alarms	Missed damage					
		A	B	C	D	E	F
PSD based	0/0/0/0	0/0/0/0	0/0/0/0	0/0/0/0	0/0/0/0	0/0/0/0	0/0/0/0
FRF based	1/0/0/ <b>35</b>	0/0/0/0	0/0/0/0	0/0/0/0	0/0/1/0	0/1/0/0	0/0/0/0
Res. varian. <sup>†</sup>	0/0/0/0	0/0/0/0	0/0/0/0	0/0/0/0	0/0/0/0	0/0/0/0	0/0/0/0
SPRT based	0/0/0/0	0/0/0/0	0/0/0/0	0/0/0/0	0/0/0/0	0/0/0/0	0/0/0/0

**False alarms** for response points Y1/Y2/Y3/Y4 out of 60 test cases per point.

**Missed damages** for response points Y1/Y2/Y3/Y4 out of 40 test cases per point; <sup>†</sup>adjusted  $\alpha$ .

Method	Damage Identification					
	Damage misclassification					
	A	B	C	D	E	F
PSD based	0/0/0/0	0/0/21/21	0/0/0/0	0/0/0/0	0/0/1/2	0/0/0/0
FRF based	0/0/0/0	<b>10/4/7/8</b>	<b>6/10/2/0</b>	<b>5/22/9/8</b>	<b>2/9/5/2</b>	<b>0/3/1/0</b>
Res. variance <sup>†</sup>	0/0/0/0	0/0/0/0	0/0/0/0	0/0/0/0	0/0/0/0	0/0/0/0
SPRT based	0/0/0/0	0/0/0/0	0/0/0/0	0/0/0/0	0/0/0/0	0/0/0/0

**Damage misclassification** for response points Y1/Y2/Y3/Y4 out of 40 test cases per point; <sup>†</sup>adjusted  $\alpha$ .

**4.2. The Frequency Response Function (FRF) based method**

This method is similar to the previous, but requires the availability of both the excitation and response signals (*excitation-response method*) and uses the FRF magnitude  $|H(j\omega)|$  (with  $j = \sqrt{-1}$ ) as its characteristic quantity (non-parametric method), thus  $Q = |H(j\omega)|$  (see Table 3). The main idea is the comparison of the FRF magnitude  $H_u(j\omega)$  of the current state of the structure to that of the healthy structure  $|H_o(j\omega)|$ . Damage detection is based on confirmation of statistically significant deviations (from the nominal/healthy) in the current FRF of the structure at one or more frequencies through a hypothesis testing problem (for each  $\omega$ ) (Fassois and Sakellariou, 2007, 2009). Damage identification may be achieved by performing a hypothesis testing similar to the above separately for damages of each potential type.

**Application Results.** Figure 6 presents typical non-parametric damage detection results via the FRF based method using the vibration measurement location of Point Y4. Evidently, correct detection at the  $\alpha = 10^{-6}$  risk level is achieved in each case, as the test statistic is shown not to exceed the critical points (dashed horizontal lines) in the healthy case, while it exceeds them in all damage cases. Again, damage types A, B and C are more easily detectable (hence more severe), while damage types D and E are harder to detect.

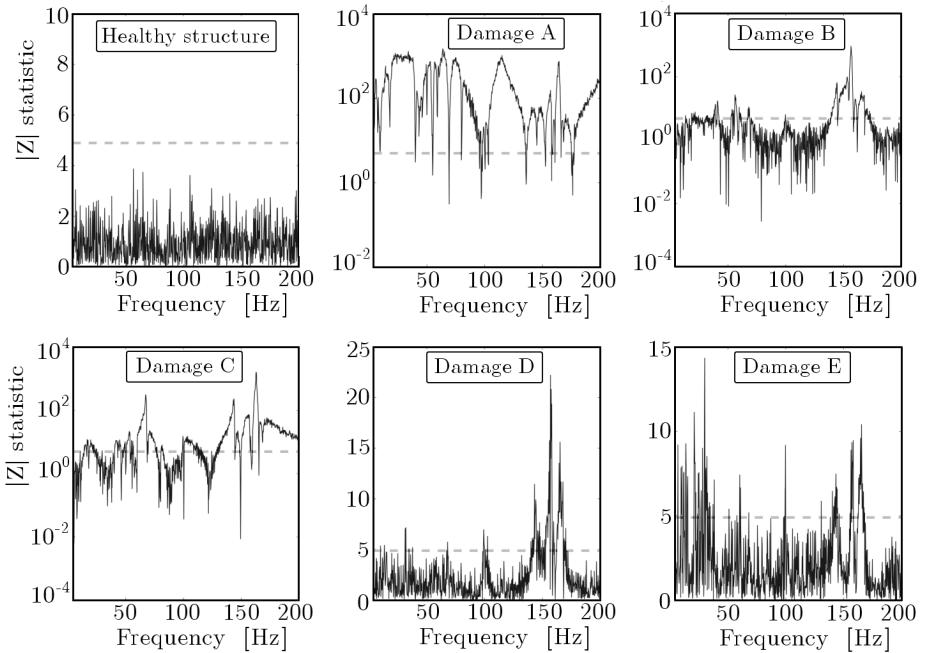


Fig. 6. FRF based method: Representative damage detection results (sensor Y4) at the  $\alpha = 10^{-6}$  risk level. The actual structural state is shown inside each plot

Representative damage identification results at the  $\alpha = 10^{-6}$  risk level using (as an example) the vibration measurement location of Point Y2 are presented in Fig. 7, with the actual damage being of type E. The test statistic does not exceed the critical point when the Damage E hypothesis is considered, while it exceeds it in all other cases. This correctly identifies damage type E as the current underlying damage.

Summary damage detection and identification results for each vibration measurement location (Fig. 1) are presented in Table 4. The FRF based method achieves effective damage detection as no false alarms or missed damages are reported (Table 4). On the other hand, the method exhibits decreased accuracy in damage identification as significant numbers of damage misclassification errors are reported for damage types B and D (Table 4).

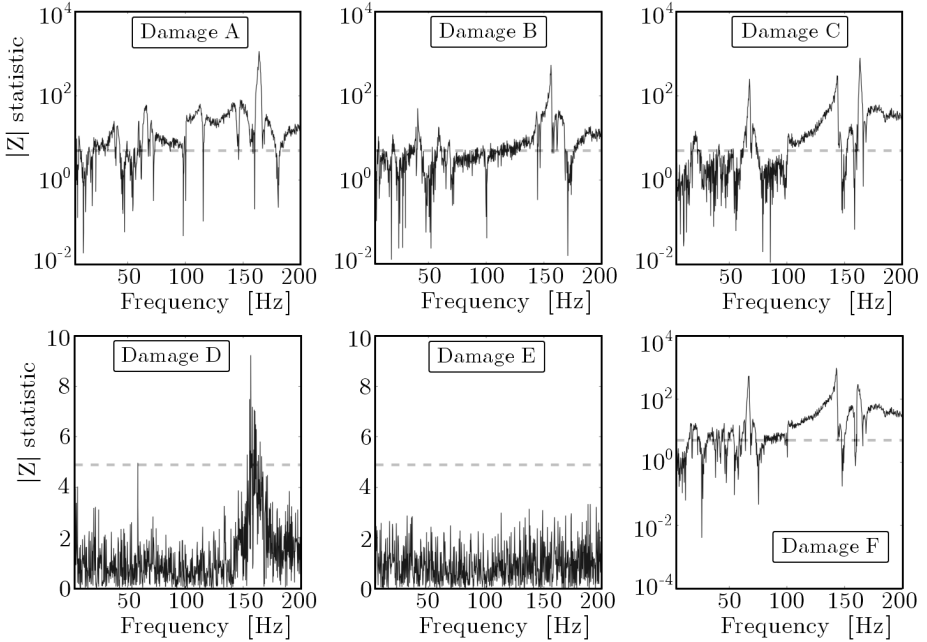


Fig. 7. FRF based method: Representative damage identification results (sensor Y2) at the  $\alpha = 10^{-6}$  risk level with the actual damage being of type E. Each considered damage hypothesis is shown inside each plot

### 4.3. The residual variance based method

In this method (*excitation-response case*) the characteristic quantity is the residual variance. The main idea is based on the fact that the model (parametric method) matching the current state of the structure should generate a residual sequence characterized by minimal variance (Fassois and Sakellariou, 2007, 2009). Damage detection is based on the fact that the residual series obtained by driving the current signal(s) through the model corresponding to the nominal (healthy) structure has a variance that is minimal if and only if the current structure is healthy (Fassois and Sakellariou, 2007, 2009). This method uses classical tests on the residuals and offers simplicity as there is no need for model estimation in the inspection phase. The main characteristics of the method are shown in Table 3.

**Application Results.** The residual variance based method employs an excitation – single response submodel obtained from the complete 4-variate VARX(80,80) models identified in the baseline phase, as well as the corresponding residual series obtained by driving the current (structure in an unknown

state) excitation and single response signals through the same submodel (inspection phase). Damage detection and identification is achieved via statistical comparison of the two residual variances.

Representative damage detection and identification results obtained via the residual variance based method (when the vibration measurement location of Point Y2 is used) are presented in Figs. 8 and 9, respectively. Evidently, correct detection (Fig. 8) is obtained in each considered case as the test statistic is shown not to exceed the critical point in the healthy case, while it exceeds it in each damage test case. Moreover, Fig. 9 demonstrates the ability of the method to correctly identify the actual damage type – in this case the vibration measurement location of Point Y3 is used.

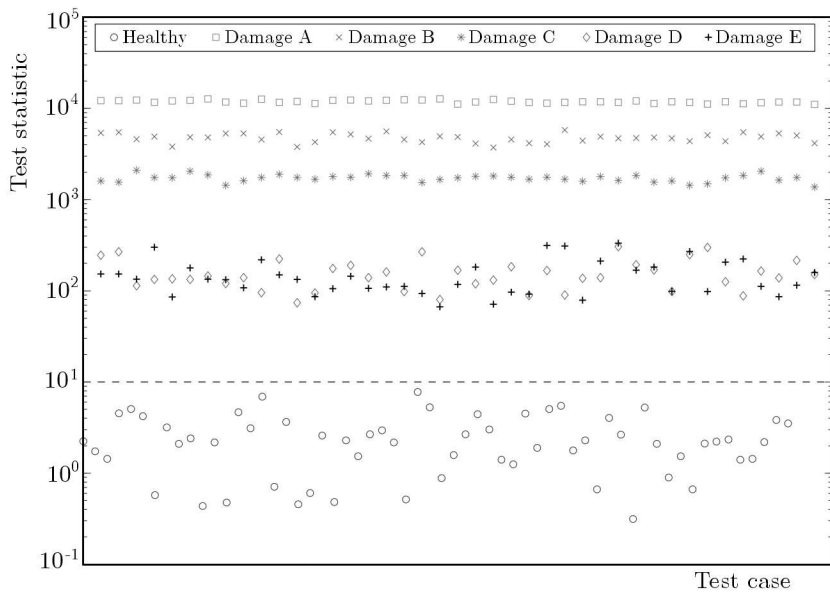


Fig. 8. Residual variance based method: Representative damage detection results (sensor Y2; healthy – 60 experiments; damaged – 200 experiments). A damage is detected if the test statistic exceeds the critical point (dashed horizontal line)

Summary damage detection and identification results for each vibration measurement location (Fig. 1) are presented in Table 4. The method achieves effective damage detection and identification as no false alarms, missed damage, or damage misclassification errors are observed.

#### 4.4. The Sequential Probability Ratio Test (SPRT) based method

This method employs the Sequential Probability Ratio Test (SPRT) (Wald, 2004; Ghosh and Sen, 1991) in order to detect a change in the standard devia-

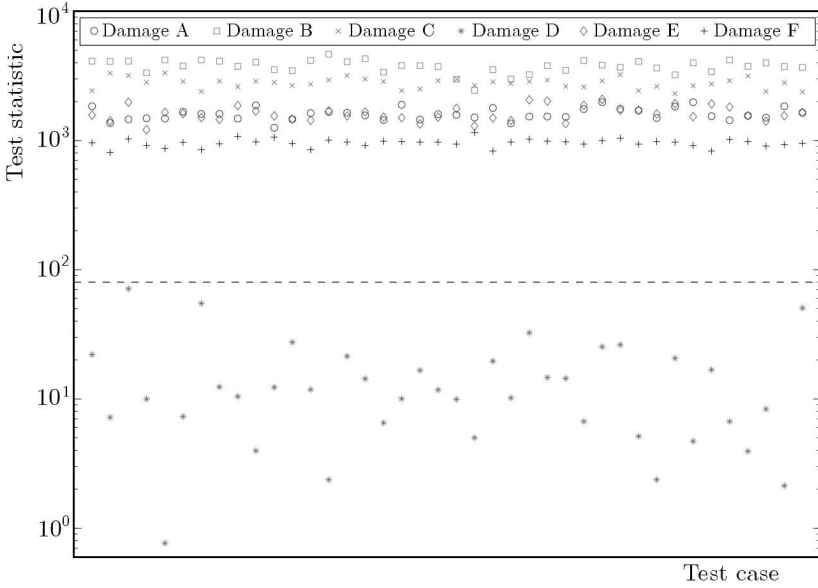


Fig. 9. Residual variance based method: Representative damage identification results (sensor Y3; 240 experiments) with the actual damage being of type D. A damage is identified as type D if the test statistic is below the critical point (dashed horizontal line)

tion  $\sigma$  of the model scalar residual sequence ( $e[t] \sim \mathcal{N}(0, \sigma^2)$ ,  $t = 1, \dots, N$ ) (parametric method). An SPRT of strength  $(\alpha, \beta)$ , with  $\alpha, \beta$  designating the type I (false alarm) and II (missed damage) error probabilities, respectively, is used for the following hypothesis testing problem:

$$\begin{aligned}
 H_o & : \sigma_{ou} \leq \sigma_o && \text{(null hypothesis – healthy structure)} \\
 H_1 & : \sigma_{ou} \geq \sigma_1 && \text{(alternative hypothesis – damaged structure)}
 \end{aligned}
 \tag{4.1}$$

with  $\sigma_{ou}$  designating the standard deviation of a scalar residual signal obtained by driving the current excitation and response signals through the healthy structural model, and  $\sigma_o, \sigma_1$  user defined values. The basis of the SPRT is the logarithm of the likelihood ratio function based on  $n$  samples

$$\begin{aligned}
 \mathcal{L}(n) & = \log \frac{f(e[1], \dots, e[n]|H_1)}{f(e[1], \dots, e[n]|H_o)} = \sum_{t=1}^n \log \frac{f(e[t]|H_1)}{f(e[t]|H_o)} \\
 & = n \log \frac{\sigma_o}{\sigma_1} + \frac{\sigma_1^2 - \sigma_o^2}{2\sigma_o^2\sigma_1^2} \sum_{t=1}^n e^2[t]
 \end{aligned}
 \tag{4.2}$$

with  $\mathcal{L}(n)$  designating the decision parameter of the method and  $f(e[t]|H_i)$

the probability density function (normal distribution) of the residual sequence under hypothesis  $H_i$  ( $i = 0, 1$ ).

The following test is then constructed at the  $(\alpha, \beta)$  risk levels:

$$\begin{aligned} \mathcal{L}(n) \leq B &\implies H_0 \text{ is accepted} && \text{(healthy structure)} \\ \mathcal{L}(n) \geq A &\implies H_1 \text{ is accepted} && \text{(damaged structure)} \\ B < \mathcal{L}(n) < A &\implies \text{no decision is made} && \text{(continue the test)} \end{aligned} \quad (4.3)$$

with  $B = \log[\beta/(1 - \alpha)]$  and  $A = \log[(1 - \beta)/\alpha]$ . Following a decision,  $\mathcal{L}(n)$  is reset to zero.

Damage identification may be achieved by performing SPRTs similar to the above separately for damages of each potential type.

**Application Results.** The SPRT based method employs an excitation – single response submodel obtained from the complete 4-variate VARX(80,80) models identified in the baseline phase as well as a corresponding residual series obtained by driving the current (structure in an unknown state) excitation and single response signals through the same submodel (inspection phase). Damage detection and identification is achieved via statistical comparison of the two residual standard deviations using the SPRT. The nominal residual standard deviation  $\sigma_o$  is selected as the mean standard deviation of the residuals obtained from the 60 healthy data sets driven through the submodel (corresponding to the selected response) of the baseline healthy VARX(80,80) model. The residual standard deviation ratio  $\sigma_1/\sigma_o$  is chosen equal to 1.1, designating a 10% increase in the nominal standard deviation (see Eqs. (4.1) and (4.2)).

Representative damage detection results at the  $\alpha = \beta = 0.01$  risk levels obtained via the SPRT based method for the vibration response (sensor) of Point Y1 are shown in Fig. 10. A damage is detected when the test statistic exceeds the upper critical point (dashed horizontal lines), while the structure is determined to be in its healthy state when the test statistic lies below the lower critical point. After a decision is made, the test statistic is reset to zero and the test continues, thus during the testing multiple decisions are made. Evidently, correct detection (Fig. 10) is obtained in each test case as the test statistic is shown to exceed multiple times (multiple correct decisions) the lower critical point in the healthy case, while it exceeds the upper critical point in the damage test cases. Observe that damage types A and C (Table 1) appear easier to detect, while damage types D and E appear harder to detect. This is in agreement with the remarks made in Subsection 3.1 and Fig. 2. Moreover, representative damage identification results at the  $\alpha = \beta = 0.01$

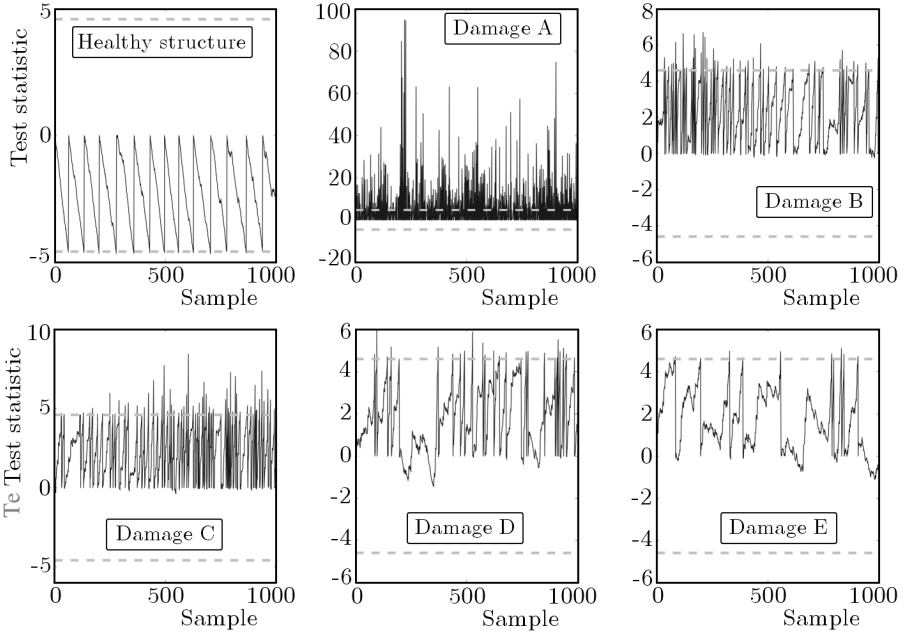


Fig. 10. SPRT based method: Representative damage detection results (sensor Y1) at the  $\alpha = \beta = 0.01$  risk levels ( $\sigma_1/\sigma_o = 1.1$ ). The actual structural state is shown inside each plot

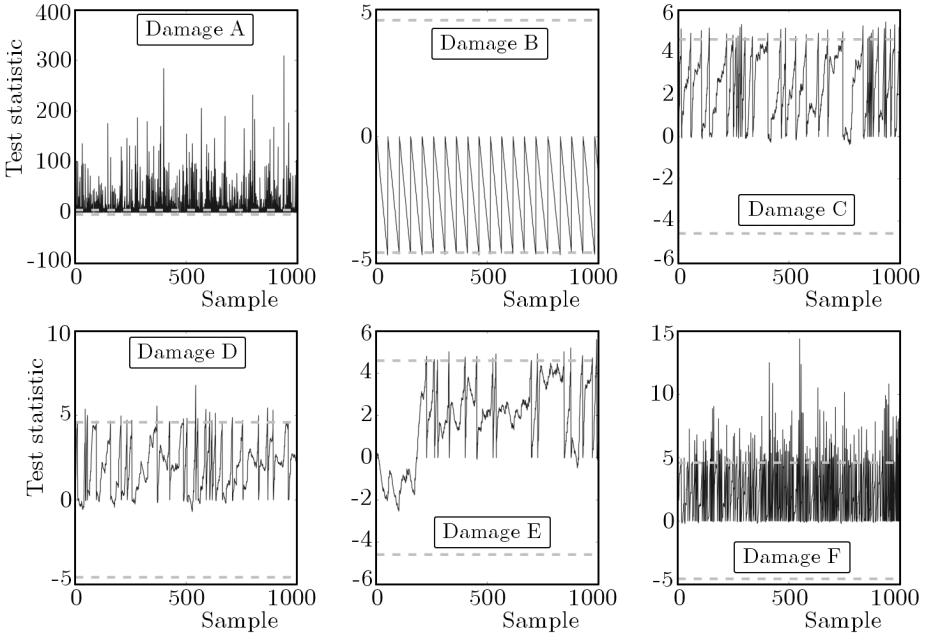


Fig. 11. SPRT based method: Representative damage identification results (sensor Y4) at the  $\alpha = \beta = 0.01$  risk levels ( $\sigma_1/\sigma_o = 1.1$ ) with the actual damage being of type B. Each considered damage hypothesis is shown inside each plot

risk levels ( $\sigma_1/\sigma_o = 1.1$ ) for the vibration measurement location of Point Y4 are depicted in Fig. 11, with the actual damage being of type B.

Summary damage detection and identification results for each vibration measurement location are presented in Table 4. The method exhibits excellent performance in damage detection and identification as no false alarms, missed damages, or damage misclassification errors are observed.

## 5. Vector time series methods and their application

Vector statistical time series methods for SHM employ *vector* (multivariate) models and corresponding statistics (Lütkepohl, 2005). Despite their phenomenal resemblance to their univariate counterparts, multivariate models generally have a much richer structure, while they typically require multivariate statistical decision making procedures (Fassois and Sakellariou, 2009; Lütkepohl, 2005). In this Section, two parametric methods, namely a model parameter based method and a residual likelihood function based method, are briefly presented and then applied to the scale aircraft skeleton structure. The main characteristics of the methods are summarized in Table 3.

### 5.1. The model parameter based method

This method treats damage detection and identification based on the characteristic quantity  $Q = \theta$  which is a function of the parameter vector  $\theta$  of a parametric time series model (Fassois and Sakellariou, 2007, 2009). In this context, the model has to be re-estimated in the inspection phase based on signals from the current (unknown) state of the structure.

Let  $\hat{\theta}$  designate a proper estimator of the parameter vector  $\theta$  (Fassois, 2001; Ljung, 1999, pp. 212-213). For sufficiently long signals, the estimator is (under mild assumptions) Gaussian distributed with mean equal to its true value  $\theta$  and a certain covariance  $\mathbf{P}_\theta$  (Ljung, 1999, p. 303), hence  $\hat{\theta} \sim \mathcal{N}(\theta, \mathbf{P}_\theta)$ .

Damage detection is based on testing for statistically significant changes in the parameter vector  $\theta$  between the nominal and current state of the structure through the hypothesis testing problem (Fassois and Sakellariou, 2007, 2009)

$$\begin{aligned} H_o & : \delta\theta = \theta_o - \theta_u = \mathbf{0} \quad (\text{null hypothesis - healthy structure}) \\ H_1 & : \delta\theta = \theta_o - \theta_u \neq \mathbf{0} \quad (\text{alternative hypothesis - damaged structure}) \end{aligned} \tag{5.1}$$

The difference between the two parameter vector estimators also follows Gaussian distribution (Fassois and Sakellariou, 2007), that is  $\delta\hat{\theta} = \hat{\theta}_o - \hat{\theta}_u \sim$

$\sim \mathcal{N}(\delta\boldsymbol{\theta}, \delta\mathbf{P})$  with  $\delta\boldsymbol{\theta} = \boldsymbol{\theta}_o - \boldsymbol{\theta}_u$  and  $\delta\mathbf{P} = \mathbf{P}_o + \mathbf{P}_u$ , where  $\mathbf{P}_o, \mathbf{P}_u$  designate the corresponding covariance matrices. Under the null ( $H_o$ ) hypothesis,  $\delta\hat{\boldsymbol{\theta}} = \hat{\boldsymbol{\theta}}_o - \hat{\boldsymbol{\theta}}_u \sim \mathcal{N}(\mathbf{0}, 2\mathbf{P}_o)$  and the quantity  $\chi_{\boldsymbol{\theta}}^2 = \delta\hat{\boldsymbol{\theta}}^\top \cdot \delta\mathbf{P}^{-1} \cdot \delta\hat{\boldsymbol{\theta}}$  (with  $\delta\mathbf{P} = 2\mathbf{P}_o$ ) follows  $\chi^2$  distribution with  $d$  (parameter vector dimensionality) degrees of freedom (Fassois and Sakellariou, 2007, 2009; Ljung, 1999, p. 558).

As the covariance matrix  $\mathbf{P}_o$  corresponding to the healthy structure is unavailable, its estimated version  $\hat{\mathbf{P}}_o$  is used. Then, the following test is constructed at the  $\alpha$  (type I) risk level:

$$\begin{aligned} \chi_{\boldsymbol{\theta}}^2 \leq \chi_{1-\alpha}^2(d) &\implies H_o \text{ is accepted} && \text{(healthy structure)} \\ \text{Else} &\implies H_1 \text{ is accepted} && \text{(damaged structure)} \end{aligned} \quad (5.2)$$

with  $\chi_{1-\alpha}^2(d)$  designating  $1 - \alpha$  critical point of the  $\chi^2$  distribution.

Damage identification may be based on multiple hypotheses testing comparing the parameter vector  $\hat{\boldsymbol{\theta}}_u$  belonging to the current state of the structure to those corresponding to different damage types  $\hat{\boldsymbol{\theta}}_A, \hat{\boldsymbol{\theta}}_B, \dots$

The main characteristics of the method are presented in Table 3.

**Application Results.** The model parameter based method employs the excitation and *all* response signals along with the *complete* 4-variate VARX(80,80) model identified in the baseline phase. In addition, a corresponding 4-variate VARX(80,80) model is identified in each test case using the current signals (inspection phase).

Figure 12 presents representative damage detection results. The healthy test statistics are shown in circles (60 experiments), while the least severe damage types D and E are presented with asterisks and diamonds, respectively (one for each one of the 40 test cases). Evidently, correct detection is obtained in each test case as the test statistic is shown not to exceed the critical point in the healthy cases, while it exceeds it in the damage cases.

Representative damage identification results (240 test cases) with the actual damage being of type F are presented in Fig. 13. Evidently, correct identification is obtained in each considered test case as the test statistics are shown not to exceed the critical point in the damage type F case, while the test cases corresponding to other damage types exceed the critical point. Note the logarithmic scale on the vertical axis which indicates significant difference between the damage type F statistics and the rest damage types statistics for the considered test cases.

Summary damage detection and identification results are presented in Table 5. The method achieves accurate damage detection and identification, as no false alarm, missed damage, or damage misclassification errors are reported.

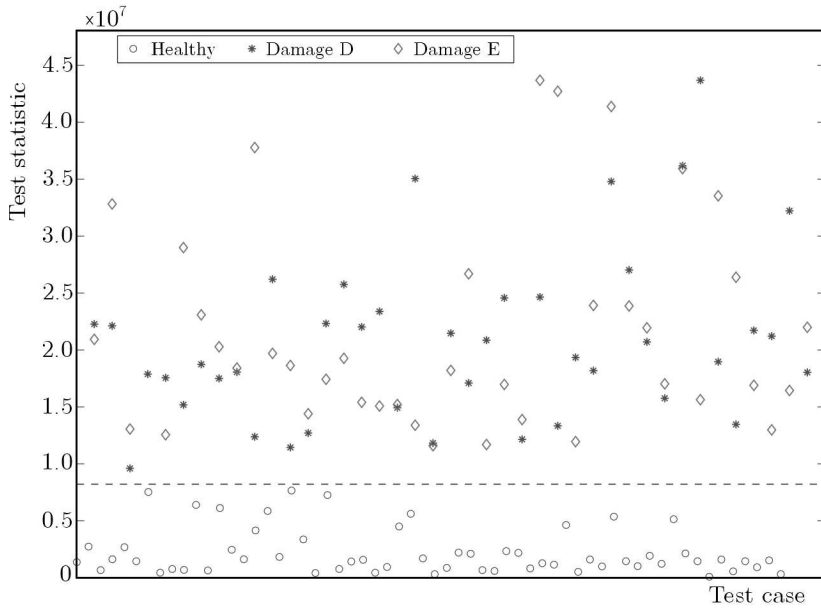


Fig. 12. Model parameter based method: Representative damage detection results for three structural states (healthy – 60 experiments; damaged – 80 experiments). A damage is detected if the test statistic exceeds the critical point (dashed horizontal line)

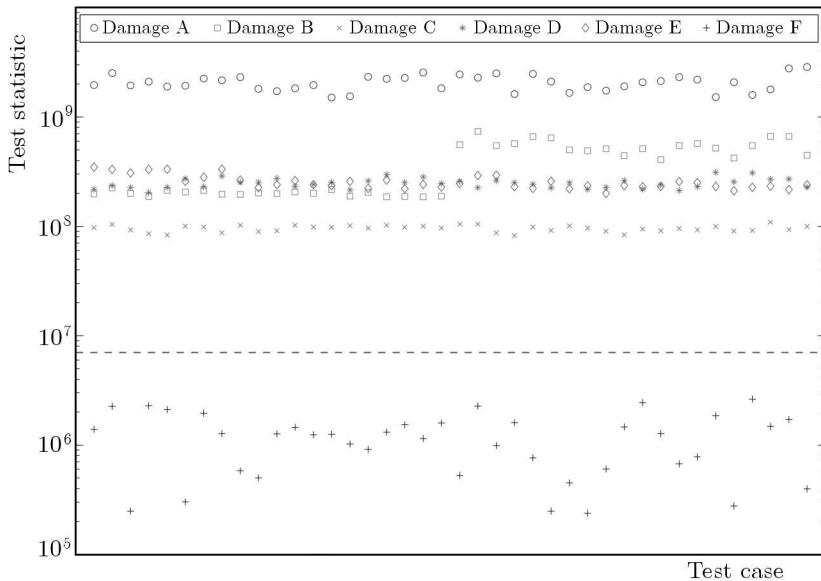


Fig. 13. Model parameter based method: Representative damage identification results (240 experiments), with the actual damage being of type F. A damage is identified as type F if the test statistic is below the critical point (dashed horizontal line)

**Table 5.** Vector methods: damage detection and identification summary results

Method	Damage Detection							Damage Identification					
	False alarms	Missed damage						Damage misclassification					
		A	B	C	D	E	F	A	B	C	D	E	F
Mod. par. <sup>†</sup>	0	0	0	0	0	0	0	0	0	0	0	0	0
Res. lik. <sup>†</sup>	0	0	0	0	0	0	0	0	0	0	0	0	0

**False alarms** out of 60 test cases. **Missed damages** out of 40 test cases.

**Damage misclassification** out of 40 test cases; <sup>†</sup>adjusted  $\alpha$ .

## 5.2. The likelihood function based method

In this method damage detection is based on the likelihood function under the null ( $H_o$ ) hypothesis of a healthy structure (Fassois and Sakellariou, 2007, 2009; Gertler, 1998, pp. 119-120). The hypothesis corresponding to the largest likelihood is selected as true for the current structural state. This method offers simplicity as there is no need for model estimation in the inspection phase.

The hypothesis testing problem considered is:

$$\begin{aligned}
 H_o &: \boldsymbol{\theta}_o = \boldsymbol{\theta}_u \quad (\text{null hypothesis - healthy structure}) \\
 H_1 &: \boldsymbol{\theta}_o \neq \boldsymbol{\theta}_u \quad (\text{alternative hypothesis - damaged structure}),
 \end{aligned} \tag{5.3}$$

with  $\boldsymbol{\theta}_o, \boldsymbol{\theta}_u$  designating the parameter vectors corresponding to the healthy and current structure, respectively. Assuming serial independence of the residual sequence, the Gaussian likelihood function  $L_y(Y, \boldsymbol{\theta}/X)$  for the data  $Y$  given  $X$  can be calculated (Fassois and Sakellariou, 2007, 2009; Box *et al.*, 1994, p. 226).

Under the null ( $H_o$ ) hypothesis, the residual series  $e_{ou}[t]$  generated by driving the current signals through the nominal (healthy) model is iid Gaussian with zero mean and covariance matrix  $\boldsymbol{\Sigma}_o$ . Decision making may be then based on the likelihood function under  $H_o$  evaluated for the current data, by requiring it to be larger or equal to a threshold  $l^*$  (which is to be selected) so that the null ( $H_o$ ) hypothesis can be accepted:

$$\begin{aligned}
 L_y(Y, \boldsymbol{\theta}_o/X) \geq l^* &\implies H_o \text{ is accepted} \quad (\text{healthy structure}) \\
 \text{Else} &\implies H_1 \text{ is accepted} \quad (\text{damaged structure})
 \end{aligned} \tag{5.4}$$

Under the null ( $H_o$ ) hypothesis the above decision making rule may be re-expressed as follows:

$$\begin{aligned}
 \sum_{t=1}^N (\mathbf{e}_{ou}^\top[t, \boldsymbol{\theta}_o] \cdot \boldsymbol{\Sigma}_o \cdot \mathbf{e}_{ou}[t, \boldsymbol{\theta}_o]) \leq l &\implies H_o \text{ is accepted (healthy struct.)} \\
 \text{Else} &\implies H_1 \text{ is accepted (damaged struct.)}
 \end{aligned}
 \tag{5.5}$$

Damage identification may be achieved by computing the likelihood function for the current signal(s) for the various values of  $\boldsymbol{\theta}$  ( $\boldsymbol{\theta}_A, \boldsymbol{\theta}_B, \dots$ ) and accepting the hypothesis that corresponds to the maximum value of the likelihood.

The main characteristics of the method are shown in Table 3.

**Application Results.** The residual likelihood function based method employs the *complete* 4-variate VARX(80,80) model identified in the baseline phase. Figure 14 shows representative damage detection results. Evidently, correct detection is obtained in each test case, as the test statistic is shown not to exceed the critical point in the healthy cases, while it exceeds it in each damage test case. Representative damage identification results, with the actual damage being of type A, are depicted in Fig. 15. Evidently, correct identification is obtained in each considered test case, as the test statistics are shown not to exceed the critical point in the damage type A case, while the test cases corresponding to the other damage types exceed the critical point.

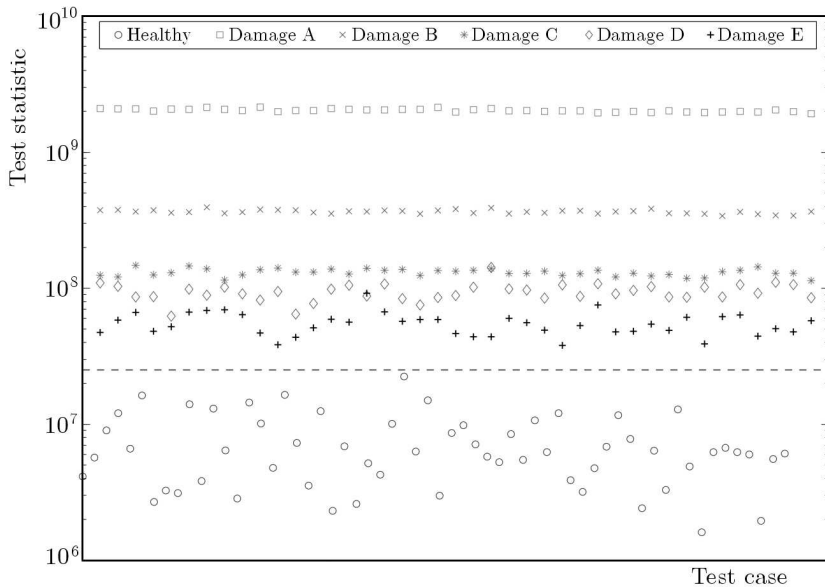


Fig. 14. Residual likelihood function based method: Representative damage detection results (healthy – 60 experiments; damaged – 200 experiments). A damage is detected if the test statistic exceeds the critical point (dashed horizontal line)

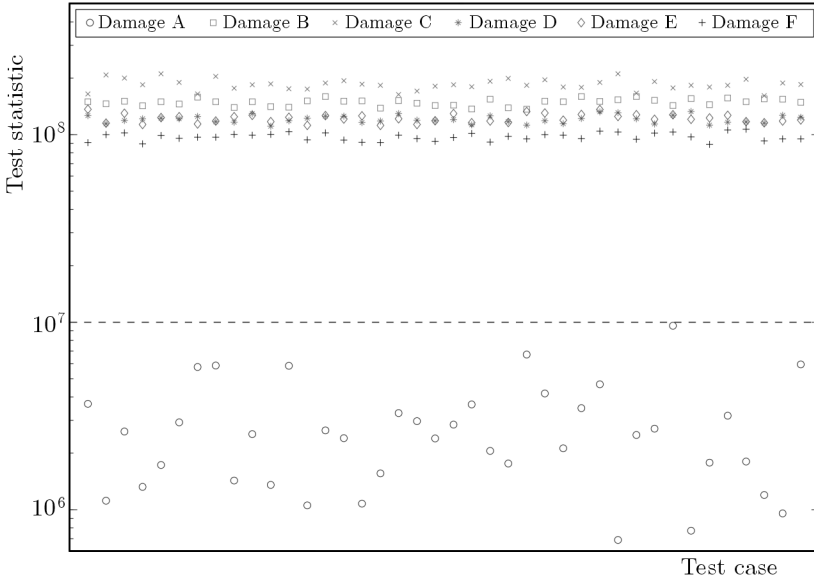


Fig. 15. Residual likelihood function based method: Representative damage identification results (240 experiments) with the actual damage being of type A. A damage is identified as type A if the test statistic is below the critical point (dashed horizontal line)

Summary damage detection and identification results are presented in Table 5. The method achieves accurate damage detection and identification as no false alarm, missed damage, or damage misclassification cases are reported.

### 6. Discussion

*Scalar* time series methods for SHM are shown to achieve effective damage detection and identification, although *non-parametric* scalar methods do seem to encounter some difficulties. The PSD based method achieves excellent damage detection, although it exhibits some misclassification errors for damage type E. The misclassification problem is more intense for damage type B when vibration measurement location Y3 or Y4 is used.

The FRF based method achieves accurate damage detection with no false alarms or missed damage errors, except for vibration measurement location Y4 for which it exhibits an increased number of false alarms. Moreover, it faces problems in correctly identifying damage types B and D, as the number of

damage misclassification errors is higher for these specific damage types. Both of these damage types involve loosening of bolts on the left wing-tip (Fig. 1). The FRF based method yields results inferior to those obtained by the PSD based method even though it employs excitation-response signals (while the latter employs response-only signals). This is probably due to the larger PSD estimate uncertainty, which seems to better “accommodate” actual structural and experimental uncertainties.

The scalar parametric residual variance and SPRT based methods achieve excellent performance in accurately detecting and identifying damage, employing any one of the vibration measurement locations (Table 4).

*Vector* time series methods for SHM achieve very accurate damage detection and identification, as with a properly adjusted risk level  $\alpha$  (type I error) no false alarm, missed damage, or damage misclassification errors are reported (Table 5). Moreover, the methods demonstrate better “global” damage detection capability. Nevertheless, parametric vector models require accurate parameter estimation and appropriate model structure (order) selection in order to accurately represent the structural dynamics and effectively tackle the damage detection and identification problems. Therefore, methods falling into this category require adequate user expertise and are somewhat more elaborate than their scalar or non-parametric counterparts.

Furthermore, the number and location of vibration measurement sensors is an important issue. Several vibration based damage diagnosis techniques that appear to work well in certain test cases could actually perform poorly when subjected to measurement constraints imposed by actual testing (Doebling *et al.*, 1998). Techniques that are to be seriously considered for implementation in the field should demonstrate that they can perform well under limitations of a small number of measurement locations and under the constraint that these locations should be selected *a priori*, without knowledge of the actual damage location. In the present study, the considered statistical time series methods have been demonstrated to be capable of achieving effective damage diagnosis based on a very limited (*vector case*) or even a single-pair (*scalar case*) of excitation-response signals. Nevertheless, their performance on large scale structures should be further investigated.

Another issue of primary importance is the proper selection of the risk level  $\alpha$  (type I error) for reasons associated with the robustness and effectiveness of the methods. If  $\alpha$  is not properly adjusted, damage diagnosis will be ineffective, as false alarm, missed damage, or damage misclassification errors may occur. The user is advised to make an initial investigation on the number of false alarms for different  $\alpha$  levels using several healthy data sets. Afterwards,

potential missed damage errors may be checked with data corresponding to various damage structural states.

Moreover, in order for certain parametric methods to work effectively, a very small value of the type I risk  $\alpha$  is often needed. This is due to the fact that the stochastic time series models (such as ARMA, ARX, state space, and so on) currently used for modeling the structural dynamics are – in reality – still incapable of fully capturing the experimental, operational and environmental uncertainties that the structure is subjected to. For this reason, a very small  $\alpha$  is often selected in order to “compensate” for the lack of effective uncertainty modeling. More accurate modeling of uncertainties is an important subject of current research (Hios and Fassois, 2009; Michaelides and Fassois, 2008).

## 7. Concluding remarks

- Statistical time series methods for SHM achieve effective damage detection and identification based on (i) random excitation and/or vibration response (*scalar* or *vector*) signals, (ii) statistical model building, and (iii) statistical decision making under uncertainty.
- Both scalar and vector statistical time series methods for SHM have been shown to effectively tackle damage detection and identification with the vector methods achieving excellent performance with zero false alarm, missed damage and damage misclassification errors.
- Both scalar and vector methods have “global” damage detection capability as they are able to detect “local” and “remote” damage (with respect to the sensor location being used).
- All methods have been shown to correctly identify the actual damage type except for the FRF based method which exhibited an increased number of damage misclassification errors for the two damage types that affect the left wing-tip of the scale aircraft skeleton structure.
- Parametric time series methods are more elaborate and require higher user expertise compared to their generally simpler non-parametric counterparts. Yet, they offer increased sensitivity and accuracy. Moreover, the vector methods based on multivariate models are more elaborate, but offer the potential of further enhanced performance.
- The availability of data records corresponding to various potential damage scenarios is necessary in order to treat damage identification. This

may be accommodated by employing scale laboratory models or tuned Finite Element models.

#### *Acknowledgement*

The authors wish to acknowledge the help of Spiros G. Magripis and Aris D. Amplianitis of the University of Patras in the experimental procedures.

### References

1. BALMES E., WRIGHT J.R., 1997, Garteur group on ground vibration testing – results from the test of a single structure by 12 laboratories in Europe, *Proceedings of ASME Design Engineering Technical Conferences*, Sacramento, U.S.A.
2. BASSEVILLE M., MEVEL L., GOURSAT M., 2004, Statistical model-based damage detection and localization: subspace-based residuals and damage-to-noise sensitivity ratios, *Journal of Sound and Vibration*, **275**, 769-794
3. BOX G., JENKINS G., REINSEL G., 1994, *Time Series Analysis: Forecasting and Control*, third edn, Prentice Hall: Englewood Cliffs, NJ
4. CARDEN E.P., BROWNJOHN J.M., 2008, ARMA modelled time-series classification for structural health monitoring of civil infrastructure, *Mechanical Systems and Signal Processing*, **22**, 2, 295-314
5. DEGENER M., HERMES M., 1996, Ground vibration test and finite element analysis of the GARTEUR SM-AG19 testbed, *Technical Report IB 232-96 J 08*, Deutsche Forschungsanstalt für Aerolastic, Göttingen
6. DOEBLING S.W., FARRAR C.R., PRIME M.B., 1998, A summary review of vibration-based damage identification methods, *Shock and Vibration Digest*, **30**, 2, 91-105
7. FASSOIS S.D., 2001, Parametric identification of vibrating structures, *Encyclopedia of Vibration*, Academic Press, 673-685
8. FASSOIS S.D., SAKELLARIOU J.S., 2007, Time series methods for fault detection and identification in vibrating structures, *The Royal Society – Philosophical Transactions: Mathematical, Physical and Engineering Sciences*, **365**, 411-448
9. FASSOIS S.D., SAKELLARIOU J.S., 2009, Statistical time series methods for structural health monitoring, [in:] *Encyclopedia of Structural Health Monitoring*, C. Boller, F.K. Chang and Y. Fujino (Eds.), John Wiley & Sons Ltd., 443-472

10. GAO F., LU Y., 2009, An acceleration residual generation approach for structural damage identification, *Journal of Sound and Vibration*, **319**, 163-181
11. GERTLER J.J., 1998, *Fault Detection and Diagnosis in Engineering Systems*, Marcel Dekker
12. GHOSH B.K., SEN P.K., EDS., 1991, *Handbook of Sequential Analysis*, Marcel Dekker, Inc., New York
13. HIOS J.D., FASSOIS S.D., 2009, Stochastic identification of temperature effects on the dynamics of a smart composite beam: assessment of multi-model and global model approaches, *Smart Materials and Structures*, **18**, 3, 035011 (15pp)
14. HWANG H.Y., KIM C., 2004, Damage detection in structures using a few frequency response measurements, *Journal of Sound and Vibration*, **270**, 1-14
15. KOPSAFTOPOULOS F.P., FASSOIS S.D., 2007, Vibration-based structural damage detection and precise assessment via stochastic functionally pooled models, *Key Engineering Materials*, **347**, 127-132
16. KOPSAFTOPOULOS F.P., FASSOIS S.D., 2010, Vibration based health monitoring for a lightweight truss structure: experimental assessment of several statistical time series methods, *Mechanical Systems and Signal Processing*, **24**, 1977-1997
17. KOPSAFTOPOULOS F.P., FASSOIS S.D., 2011, Statistical time series methods for damage diagnosis in a scale aircraft skeleton structure: loosened bolts damage scenarios, *Proc. of the 9th International Conference on Damage Assessment of Structures (DAMAS 2011)*, University of Oxford, England
18. KOPSAFTOPOULOS F.P., MAGRIPIS S.G., AMPLIANITIS A.D., FASSOIS S.D., 2010, Scalar and vector time series methods for vibration based damage diagnosis in an aircraft scale skeleton structure, *Proc. of the ASME 2010 10th Biennial Conference on Engineering Systems Design and Analysis*, Istanbul, Turkey
19. LIBERATORE S., CARMAN G.P., 2004, Power spectral density analysis for damage identification and location, *Journal of Sound and Vibration*, **274**, 3/5, 761-776
20. LJUNG L., 1999, *System Identification: Theory for the User*, 2nd edn, Prentice-Hall
21. LÜTKEPOHL H., 2005, *New Introduction to Multiple Time Series Analysis*, Springer-Verlag Berlin
22. MATTSON S., PANDIT S., 2006, Statistical moments of autoregressive model residuals for damage localization, *Mechanical Systems and Signal Processing*, **20**, 627-645
23. MICHAELIDES P.G., FASSOIS S.D., 2008, Stochastic identification of structural dynamics from multiple experiments – experimental variability analysis, *Proceedings of the ISMA Conference on Noise and Vibration Engineering*, Leuven, Belgium

24. NAIR K.K., KIREMIDJIAN A.S., LAW K.H., 2006, Time series-based damage detection and localization algorithm with application to the ASCE benchmark structure, *Journal of Sound and Vibration*, **291**, 349-368
25. RIZOS D.D., FASSOIS S.D., MARIOLI-RIGA Z.P., KARANIKA A.N., 2008, Vibration-based skin damage statistical detection and restoration assessment in a stiffened aircraft panel, *Mechanical Systems and Signal Processing*, **22**, 315-337
26. SAKELLARIOU J.S., FASSOIS S.D., 2006, Stochastic output error vibration-based damage detection and assessment in structures under earthquake excitation, *Journal of Sound and Vibration*, **297**, 1048-1067
27. SAKELLARIOU J.S., FASSOIS S.D., 2008, Vibration based fault detection and identification in an aircraft skeleton structure via a stochastic functional model based method, *Mechanical Systems and Signal Processing*, **22**, 557-573
28. SAKELLARIOU J.S., PETSOUNIS K.A., FASSOIS S.D., 2001, Vibration analysis based on-board fault detection in railway vehicle suspensions: a feasibility study, *Proceedings of First National Conference on Recent Advances in Mechanical Engineering*, Patras, Greece
29. SOHN H., ALLEN D.W., WORDEN K., FARRAR C.R., 2003, Statistical damage classification using sequential probability ratio tests, *Structural Health Monitoring*, **2**, 1, 57-74
30. SOHN H., FARRAR C.R., 2001, Damage diagnosis using time series analysis of vibration signals, *Smart Materials and Structures*, **10**, 446-451
31. SOHN H., FARRAR C.R., HUNTER N.F., WORDEN K., 2001, Structural damage classification using extreme value statistics, *Journal of Dynamic Systems, Measurement, and Control*, **127**, 125-132
32. WALD A., 2004, *Sequential Analysis*, Dover Publications Inc., New York
33. ZHENG H., MITA A., 2007, Two-stage damage diagnosis based on the distance between ARMA models and pre-whitening filters, *Smart Materials and Structures*, **16**, 1829-1836

## Skalarne i wektorowe szeregi czasowe w diagnostyce uszkodzeń opartej na analizie drgań na przykładzie modelu szkieletu samolotu

### Streszczenie

W pracy zawarto analizę porównawczą kilku skalarnych i wektorowych statystycznych szeregów czasowych stosowanych w technikach monitorowania stanu konstrukcji (SHM) na podstawie ich skuteczności w zastosowaniu do wykrywania uszkodzeń szkieletowej struktury laboratoryjnego modelu samolotu dla różnych scenariuszy

uszkodzeń wywołanych poluzowaniem połączeń śrubowych. Zaprezentowano krótki przegląd skalarnych i wektorowych metod analizy, tj. bazujących na skalarnych i wektorowych sygnałach i statystykach, oraz odpowiadające im modele. Metody te sklasyfikowano jako nieparametryczne i parametryczne oraz oparte wyłącznie na informacji o odpowiedzi dynamicznej układu lub relacji pomiędzy wymuszeniem i odpowiedzią. Efektywność rozważanych metod oceniono na podstawie kilku eksperymentalnych przypadków badawczych odpowiadających różnym scenariuszom uszkodzeń modelu. Wyniki badań ujawniły różne aspekty zastosowanych technik analizy i potwierdziły przydatność skalarnych i wektorowych szeregów czasowych w diagnostyce i monitorowaniu stanu konstrukcji (SHM).

*Manuscript received March 1, 2011; accepted for print June 2, 2011*